Available online at www.sciencedirect.com
SCIENCE DIRECT
Journal of Solid State Chemistry 179 (2006) 1768–1774
JOURNAL OF SOLID STATE CHEMISTRY
www.elsevier.com/locate/jssc

Ferroelectric and dielectric properties of bismuth-layered structural $Sr_2Bi_{4-x}Ln_xTi_5O_{18}$ (Ln = La, Nd, Sm and Dy) ceramics

Feng Qiang[a], Jun-Hui He[a], Jun Zhu[a], Xiao-Bing Chen[a,b,*]

[a]College of Physics Science and Technology, Yangzhou University, Yangzhou 225002, China
[b]National Laboratory of Solid State Microstructures, Nanjing University, Nanjing 210008, China

Received 13 September 2005; received in revised form 16 February 2006; accepted 16 March 2006
Available online 24 April 2006

Abstract

La, Nd, Sm, and Dy-doped $Sr_2Bi_4Ti_5O_{18}$ (SBTi) ceramic samples have been prepared by the solid-state reaction method. The X-ray diffraction reveals that all of the ceramic samples are single phase compounds. Their remnant polarization ($2P_r$) increases at first, and then decreases with the increase of doping content. When doping content is 0.01, Sm and Dy-doped SBTi samples exhibit the maximum $2P_r$ of 18.2 and 20.1 μC/cm^2, respectively. While La and Nd-doped SBTi samples display the maximum $2P_r$ value of 18.4 and 19.1 μC/cm^2 with doping content of 0.05 and 0.10, respectively. The ferroelectric properties of $Sr_2Bi_{4-x}Ln_xTi_5O_{18}$ are found to be dominated by the competition of the decrease of oxygen vacancy concentration and the relief of structural distortion.

Keywords: Ceramics; Dielectric properties; Ferroelectricity

1. Introduction

Ferroelectric materials have been intensively studied for their application to nonvolatile ferroelectric random access memories (FeRAMs) [1,2]. In order to meet the requirements for such memory applications, ferroelectric capacitors should have large remnant polarization, low coercive field, good fatigue endurance and thermal stability [3]. ABO_3 type ferroelectric Pb(Zr,Ti)O_3 (PZT) has the advantage of large polarization value ($2P_r$ = 20–70 μC/cm^2), but has the drawbacks of poor fatigue endurance and high coercive field [3–5]. Considerable attention has been recently paid to bismuth layer-structured ferroelectrics (BLSFs) as ferroelectric materials instead of conventional lead-based ferroelectrics because of its excellent fatigue properties and Pb-free chemical composition. BLSFs are generally formulated as $(Bi_2O_2)^{2+}(A_{m-1}B_mO_{3m+1})^{2-}$, where A is mono-, di-, or trivalent ions, B is tetra-, penta-, or hexavalent ions with appropriate size, and m (m = 1, 2, 3, 4 and 5) is the number of BO_6 octahedra in the perovskite blocks $(A_{m-1}B_mO_{3m+1})^{2-}$, sandwiched between bismuth oxide layers $(Bi_2O_2)^{2+}$ along the c-axis [6,7]. $SrBi_2Ta_2O_9$ (SBT), which is within the family of BLSFs (m = 2), has good fatigue endurance and low coercive field, but small polarization ($2P_r$ = 4–16 μC/cm^2) [3,8]. $Bi_4Ti_3O_{12}$ (BIT, m = 3) is an attractive candidate for FeRAMs because of its large spontaneous polarization. However, BIT thin film shows fatigue and unexpectedly low value of $2P_r$ (4–8 μC/cm^2) [3].

Recently, $Sr_2Bi_4Ti_5O_{18}$ (SBTi) compound has been widely noticed and investigated due to its promising application for FeRAMs [9]. SBTi is a kind of typical material of BLSFs with m = 5. SBTi thin film was reported to show excellent retention characteristics after 10^5 s and almost no fatigue at least up to 10^{11} cycles, with a saturated polarization ($2P_s$) value of 29.2 μC/cm^2. However, the remnant polarization ($2P_r$) value of SBTi thin film is only 10 μC/cm^2 at an applied field of 200 kV/cm [9]. To meet the application of high-density FeRAMs, the $2P_r$ of SBTi ought to be enlarged.

Several investigations suggested that the defects such as oxygen vacancies would accumulate near the domain boundaries and result in strong domain pinning, which leads to a small $2P_r$ [10,11]. Thus, it is believed that the

*Corresponding author. College of Physics Science and Technology, Yangzhou University, Yangzhou 225002, China.
E-mail address: xbchen@yzu.edu.cn (X.-B. Chen).

0022-4596/$ - see front matter © 2006 Elsevier Inc. All rights reserved.
doi:10.1016/j.jssc.2006.03.012

control of defects in the perovskite blocks or Bi_2O_2 layers is essential to obtain large remnant polarization. Many investigations on BIT indicated that substitution of stable trivalent ions for volatile bismuth ions was effective for suppressing oxygen vacancy concentration and increasing the chemical stability of the perovskite layers. For instance, the $2P_r$ of La-doped BIT ceramics and films were obviously increased [3]. In addition, Chon et al. reported that the Sm-doped BIT ($Bi_{4-x}Sm_xTi_3O_{12}$) thin films show excellent fatigue-free characteristics and very large $2P_r$ of 49 μC/cm^2 as $x = 0.85$ [12].

In this paper, SBTi ceramic samples with Bi^{3+} at *A*-site substituted by La, Nd, Sm and Dy ions have been prepared by the solid-state reaction method. The $2P_r$ of $Sr_2Bi_{4-x}Ln_xTi_5O_{18}$ (*Ln* = La, Nd, Sm and Dy) is obviously increased in comparison with that of undoped SBTi ceramic. And the coercive field (E_c) of SBTi is decreased.

2. Experiments

Ceramic samples of $Sr_2Bi_{4-x}Sm_xTi_5O_{18}$ (SBST, $x = 0.00$, 0.01, 0.05, 0.15, 0.25 and 0.50), $Sr_2Bi_{4-x}Dy_xTi_5O_{18}$ (SBDT, $x = 0.00$, 0.01, 0.05, 0.15 and 0.20), $Sr_2Bi_{4-x}La_xTi_5O_{18}$ (SBLT, $x = 0.00$, 0.01, 0.05, 0.15 and 0.20) and $Sr_2Bi_{4-x}Nd_xTi_5O_{18}$ (SBNT, $x = 0.00$, 0.05, 0.10, 0.15, 0.20 and 0.25) were prepared by the solid-state reaction method. Stoichiometric amounts of $SrCO_3$, Bi_2O_3, TiO_2, Sm_2O_3, Dy_2O_3, La_2O_3 and Nd_2O_3 powders with 99+% purity were used as the starting materials. To compensate bismuth vaporization during sintering process, excess Bi_2O_3 up to 5 wt% was added into the starting powder. The powders were firstly mixed by ball milling for 24 h, and then were calcined at 860–870 °C for 8 h. To obtain the dense samples, the calcined powder was crushed thoroughly and pressed into pellets. Then the pellets were sintered in air at 1180–1190 °C for 4 h followed by furnace cooling.

The crystal structures of the SB*Ln*T (*Ln* = Sm, Dy, La and Nd) ceramics were determined by X-ray diffraction (XRD) method using an M03XHF22 X-ray diffractometry with Cu*K*α radiation ($\lambda = 0.154056$ nm) at a tube voltage of 40 kV and a tube current of 40 mA. The microstructure and surface morphology of the ceramics were investigated using an XL-30ESEM scanning electron microscope (SEM). The pellets were filed and polished to a thickness of about 0.3 and 0.5 mm, then electroded with silver for ferroelectric and dielectric property measurements. The ferroelectric hysteresis loops were measured at room temperature using a Precision LC ferroelectric tester (Radiant Technologies, Inc). The temperature dependence of the dielectric constant (ε) and dielectric loss ($\tan\delta$) were measured with an HP-4192A low frequency impedance analyzer.

3. Results and discussion

The XRD patterns reveal that all of the samples are in the single phase of BLSFs crystal structure. Fig. 1 shows typical XRD patterns of the SBTi, SBST-0.01, SBDT-0.01, SBLT-0.05 and SBNT-0.10 samples whose remnant polarization are obviously improved. The coincidence of the XRD patterns are related to the equality of the chemical valence and the closed ions radii between the Ln^{3+} and Bi^{3+} ions [13]. The cell parameter of SBTi, *a*, *b*, and *c* is 3.857(7) Å, 3.854(8) Å, and 48.828(1) Å, respectively. The structure of SBTi is orthorhombic in space group *B*2*ab*.

Fig. 2 displays the ferroelectric hysteresis loops of SBTi, SBST-0.01, SBDT-0.01, SBLT-0.05, SBNT-0.10 and SBDT-0.15 ceramics under a driven electric field of about 125 kV/cm. The $2P_r$ of SBTi ceramic at zero *Ln*-doping content is about 16.3 μC/cm^2, larger than that of SBTi thin films (10 μC/cm^2). Fig. 3(a) presents the dependence of the remnant polarization of the SB*Ln*T samples on the *Ln* content (*x*). The error of the $2P_r$ is within 5%. It is noticed that the $2P_r$ increases at first, then decreases with the increase of doping content. When doping content is 0.01, the $2P_r$ for Sm and Dy-doped SBTi exhibit a maximum value of 18.2 and 20.1 μC/cm^2, respectively. While the maximum $2P_r$ of La (18.4 μC/cm^2) and Nd (19.1 μC/cm^2) doped SBTi appears at the content of 0.05 and 0.10, respectively. However, as shown in Fig. 3(b), the E_c decreases monotonously with increasing *Ln*-doping. The error of the E_c is within 3%. Above results indicate that Ln-doping with appropriate content can improve the ferroelectric property of SBTi.

The dielectric properties for SB*Ln*T samples were measured at a frequency of 500 kHz from room temperature to 350 °C. Fig. 4 shows the temperature dependence of dielectric constant ε for SBST and SBDT samples. The ε–*T* curves for SBNT is similar to that for SBST. The dielectric behaviors of SBLT have been reported in our previous

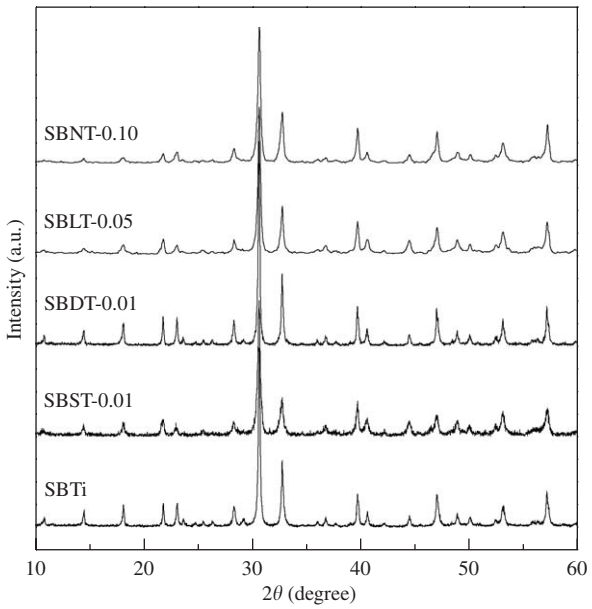

Fig. 1. XRD patterns of SBTi, SBST-0.01, SBDT-0.01, SBLT-0.05 and SBNT-0.10 ceramics.

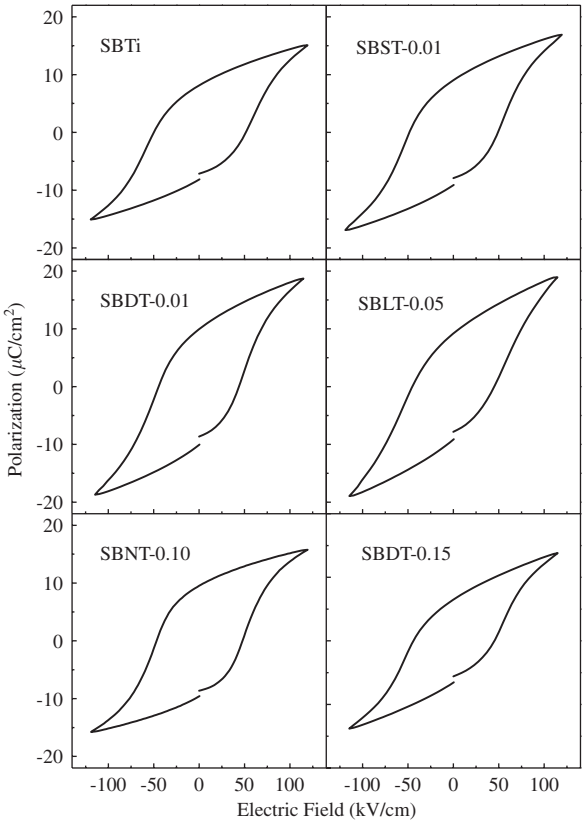

Fig. 2. Ferroelectric hysteresis loops of SBTi, SBST-0.01, SBDT-0.01, SBLT-0.05, SBNT-0.10 and SBDT-0.15 ceramic samples.

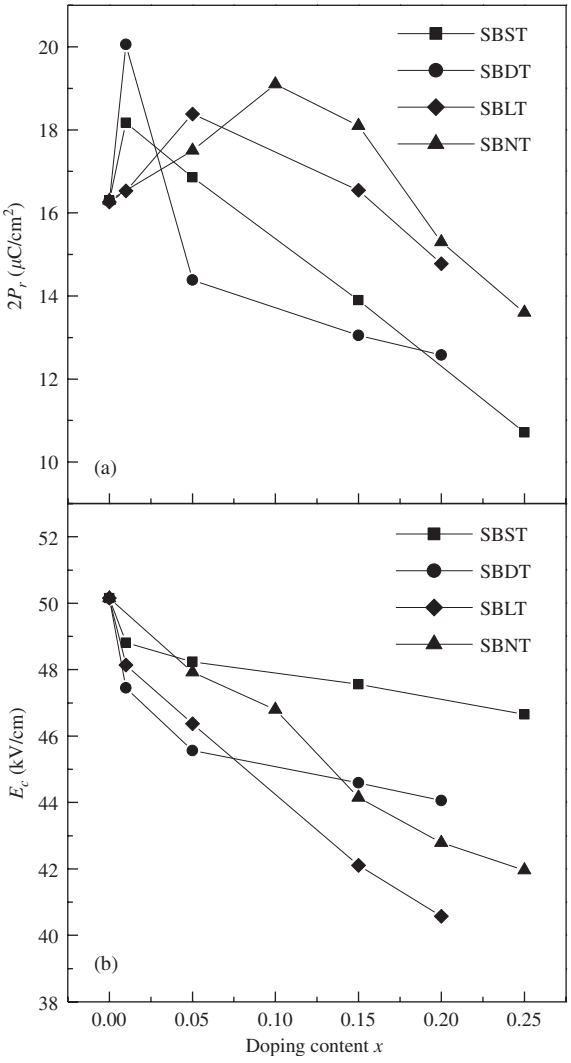

Fig. 3. Dependence of (a) $2P_r$ and (b) E_c on the doping content x at room temperature.

work [14]. In ε–T curves, Curie temperature (T_c) could be evaluated from the temperature at maximum value of ε.

From Fig. 4(a) and (b), SBTi and the samples with low Sm or Dy-doping content show the rather sharp dielectric peaks. While upon higher Sm or Dy-doping, the dielectric transition peaks become broadened obviously. La or Nd-doping broadens the dielectric peak in ε–T curves similarly. The broadening of dielectric peaks may be attributed to the difference of the ionic radii between Ln^{3+} and Bi^{3+}. In $Bi_4Ti_3O_{12}$, $SrBi_4Ti_4O_{15}$, or intergrowth $Bi_4Ti_3O_{12}$–$SrBi_4Ti_4O_{15}$, it is generally accepted that La ions are incorporated into the A-site as the doping content is low, which has been confirmed by Raman experiments [15–17]. Since the ionic radius of La^{3+}/Nd^{3+}/Sm^{3+}/Dy^{3+} is smaller than that of Bi^{3+} (La^{3+}: 1.160 Å, Nd^{3+}: 1.109 Å, Sm^{3+}: 1.079 Å, Dy^{3+}: 1.027 Å, Bi^{3+}: 1.170 Å) [13], the exchange of the cations between Bi in Bi_2O_2 layers and La/Nd/Sm/Dy in A-sites would occur for samples with higher doping content to release the size mismatch between Bi_2O_2 layers and perovskite blocks [18]. Thus, cations at A-site distributed in a microscopic scale are inhomogeneous, which leads to microscopic ferroelectric domains with slightly different T_c values. The distribution of T_c induces the dispersion of the phase-transition, indicated by the broadening of the dielectric peaks [18].

The ε value at T_c for SBTi is about 1470, in agreement with that reported by Srinivas [19]. For SBST-0.01 and SBDT-0.01, ε is increased to the value of 1554 and 1769, respectively, which suggest that higher ε at T_c could be achieved by small amount of doping into SBTi. For $x \geqslant 0.01$, the ε begins to decrease with increasing Sm or Dy-doping content, which may arise from the change of grain size caused by Ln-doping [20,21]. The SEM photographs for surface morphology of SBTi, SBST-0.01, SBST-0.15 and SBST-0.50 ceramics are displayed in Fig. 5. It can be noticed that the SBTi and SBST-0.01 samples exhibit similar grain sizes. However, upon higher Sm-doping content the grain size tends to be decreased gradually. The decrease of dielectric constant may be related to the smaller grain size [20,22].

The T_c of SBTi is measured to be 286.7 °C, while the T_c of the SBLnT samples shifts to lower temperatures monotonously with Ln-doping, as shown in Fig. 6. It is generally accepted that the decrease of T_c implies the relief of structural distortion [23]. Because there exists strong hybridization between Bi 6s and O 2p orbit, Bi^{3+} ions with lone-pair 6s electrons tend to be covalently bonded with

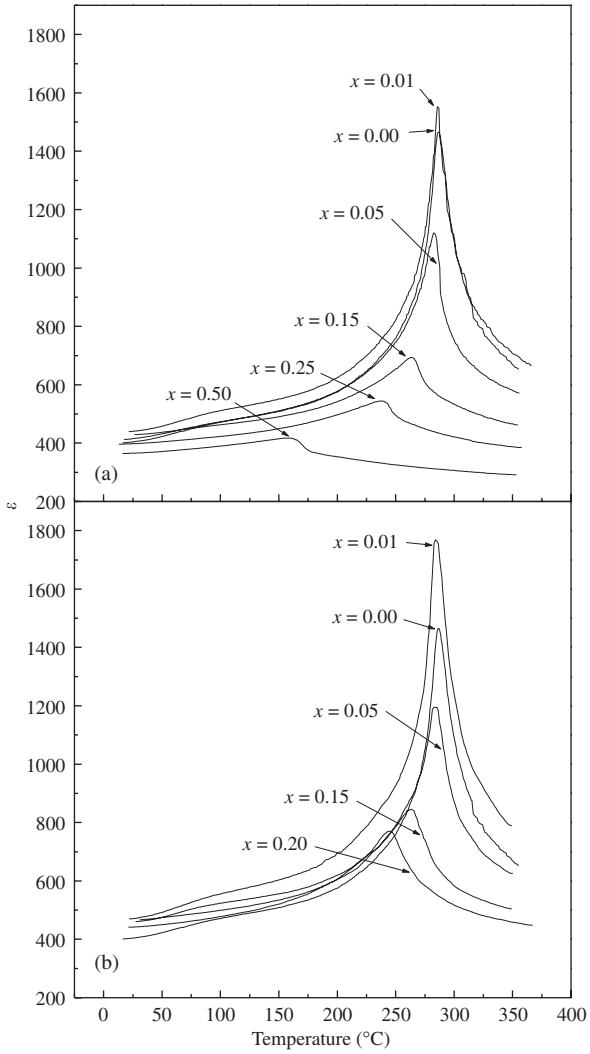

Fig. 4. The temperature dependence of dielectric constant ε of (a) SBST, and (b) SBDT samples at 500 kHz.

O^{2-} ions, which leads to a drastic distortion of the pseudo-perovskite blocks [24,25]. On the contrary, when lanthanide ion without 6*s* electrons occupies the *A*-site, the structural distortion relives, which leads to the decrease of T_c. Among doping ions, La-doping decreases the T_c more drastically than Nd, Sm and Dy-doping. This likely arises from the difference of their outer electronic configurations. As well known, there is no 4*f* electron in $La^{3+}(5s^25p^6)$ ions, whereas the 4*f* orbits of $Nd^{3+}(4f^45s^25p^6)$, $Sm^{3+}(4f^65s^25p^6)$ and $Dy^{3+}(4f^{10}5s^25p^6)$ ions are occupied by uncoupled electrons. Although the special distribution of 4*f* electron orbit in *Ln* ions is denser than that of 6*s* orbit in Bi^{3+} ion, the hybridization between 4*f* electrons of Nd^{3+}, Sm^{3+}, Dy^{3+} and 2*p* electrons of O^{2-} might occur to a certain extent. But in the case of La-doped SBTi, such hybridization does not exist due to the absence of 4*f* electron, which considerably favors to the relief of the structure distortion. Therefore the T_c of La-doped SBTi decreases more drastically than that of Nd, Sm and Dy-doped SBTi.

On the other hand, the Coulomb interaction between Ln^{3+} ions and O^{2-} ions, which is dependent on effective nuclear charge of Ln^{3+} ions, may also exert certain influence on the relief of the structure distortion. Generally, the number of effective nuclear charge Z' for lanthanide ions can be calculated by [26]

$$Z' = Z - n_0 - \sigma \times n_f,$$

where Z is the atomic number, n_0 is the number of inner electrons, σ is the shielding constant of *f* electrons, and n_f is the number of *f* electrons in ions. For lanthanide, the value of n_0 and σ are 46 and 0.85, respectively. The calculated Z' are given in Table 1, where Z' value increases with the atomic number. Thus the Coulomb interaction between La^{3+} ions and O^{2-} ions is estimated to be the least strong among the four doping lanthanide. As a whole, both the relatively weak Coulomb interaction and hybridization interaction may favor to the relief of the structure distortion for La-doped SBTi, which brings about more drastic decrease of T_c.

Fig. 7 shows the temperature dependence of dielectric loss for SBST and SBDT at 500 kHz. In the dielectric loss curves, three dielectric loss peaks marked with P_1, P_2 and P_3 are observed. As shown in Fig. 7(a), P_1 and P_2 peaks decrease obviously with Sm-doping, and almost disappear as Sm content reaches 0.50. Previous investigation suggested that the decreases of P_1 and P_2 peaks are caused by the concentration decrease of point defects such as oxygen vacancies [27]. The formation of these oxygen vacancies is related to the Bi vaporization. The present results indicate that Sm-doping may suppress the formation of the defects, and hence result in the weakening of P_1 and P_2 peaks. P_3 peak is generally considered to be related to the viscous motion of domain walls [27]. Therefore, the decrease of the P_3 peak with Sm-doping implies the increase of the mobility of domain walls. In addition, when $x > 0.25$, the influence of Sm-doping on the P_3 peak becomes negligible. In Fig. 7(b), the P_1, P_2 and P_3 peaks of SBDT samples decrease with Dy-doping when $x \leqslant 0.15$, which is analogous to the situation in SBST. However, the P_3 peak of SBDT-0.20 becomes higher than that of SBDT-0.15. For SBLT and SBNT samples, the dielectric loss factor ($\tan\delta$) decreases obviously with La and Nd-doping, similar to Sm and Dy-doping. Above results indicate that *Ln*-doping can obviously suppress the occurrence of defects.

The remnant polarization of *Ln*-doped SBTi is considered to be dominated by the competition of the decrease of oxygen vacancy concentration and the relief of structural distortion. *Ln*-doping at the *A*-site in SBTi would lower the concentration of oxygen vacancies and improve the chemical stability of the perovskite blocks and Bi_2O_2 layers. The elimination of oxygen vacancies is helpful to weaken the influence of domain pinning and result in the increase of the $2P_r$. Nevertheless, *Ln*-doping leads to the decrease of T_c, which suggests that the structural distortion of SB*Ln*T relieves with *Ln*-doping. Generally in displacive

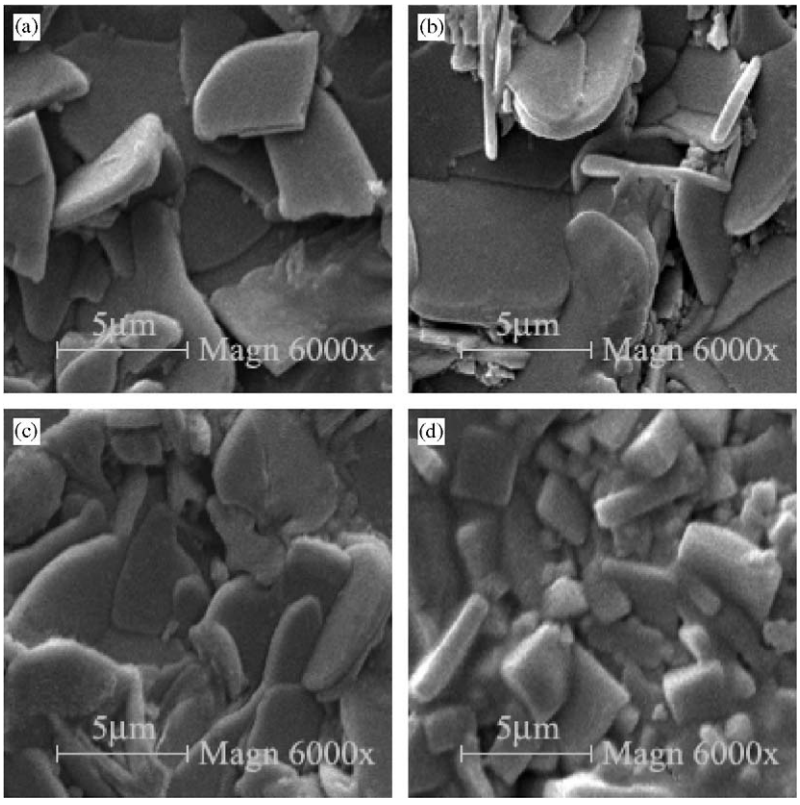

Fig. 5. SEM images of (a) SBTi, (b) SBST-0.01, (c) SBST-0.15, and (d) SBST-0.50 ceramics.

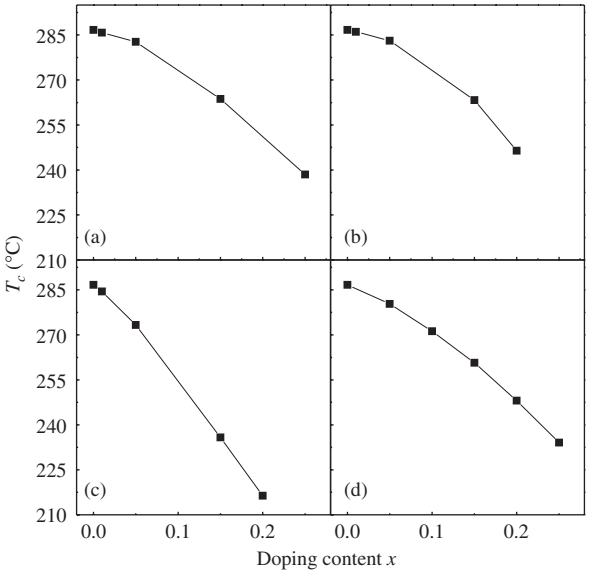

Fig. 6. The T_c for (a) SBST, (b) SBDT, (c) SBLT, and (d) SBNT as a function of doping content x.

ferroelectrics, the relaxation of the structure brings about a decrease in spontaneous polarization (P_s) [23]. Therefore, *Ln*-doping would cause the decrease of $2P_r$. When doping content is low, the influence of lanthanide on structural distortion is negligible, and the increase of $2P_r$ is mainly caused by the weakening of the domain pinning. For higher *Ln* content, the influence of structural distortion on the $2P_r$ becomes more significant, which becomes a dominating factor and decreases $2P_r$.

Table 1
The number of effective nuclear charge Z' for doping ions by calculation

Ion	Z	n_f	Z'
La^{3+}	57	0	11.00
Nd^{3+}	60	3	11.45
Sm^{3+}	62	5	11.75
Dy^{3+}	66	9	12.35

Based on above results, a critical *Ln*-doping range may exist between 0.01 and 0.10 in SBTi. In the La-doped BIT ($Bi_{4-x}La_xTi_3O_{12}$) system and La-doped $SrBi_4Ti_4O_{15}$ ($SrBi_{4-x}La_xTi_4O_{15}$) system, the $2P_r$ reaches a maximum value when x is about 0.75 and 0.25, respectively [3,14]. These two values of the critical content are much larger than that of lanthanide-doping in SBTi. It is assumed that the more stable Sr^{2+} ions at *A*-site act as lanthanide ions and decrease the acceptability of lanthanide ions into perovskite blocks. So the lanthanide content at the maximum value of $2P_r$ decreases with the increasing concentration of Sr^{2+} ions. With the higher doping content, lanthanide ions are incorporated into not only the perovskite layers but also the Bi_2O_2 layers [15]. As widely accepted, Bi_2O_2 layers, acting as an insulating layer

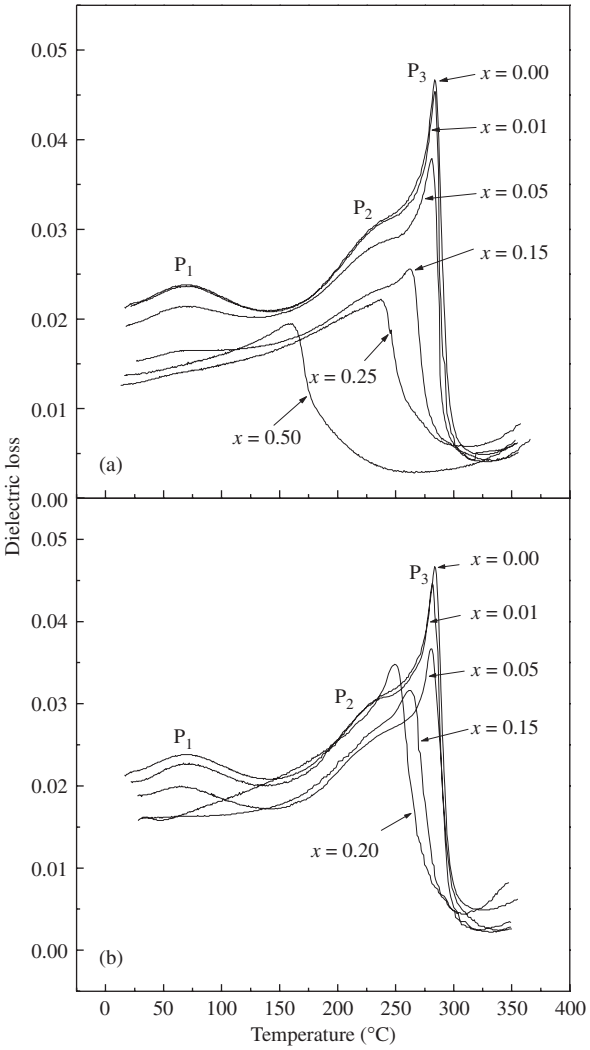

Fig. 7. The temperature dependence of the dielectric loss for (a) SBST, and (b) SBDT at 500 kHz.

and space charge storage, play an important role for the ferroelectric properties of BLSFs [25]. The incorporation of lanthanide ions into Bi_2O_2 layer might leads to the loss of its original function, deteriorating the ferroelectric property. This may be another possible reason for the decease of the $2P_r$.

As to the influence of *Ln*-doping on E_c, the ionic radii of *Ln* and the lattice distortion may play an important role. Since the radii of doping ions is smaller than that of Bi^{3+}, the displacement of the polar ions in SB*Ln*T becomes easier than that in SBTi ceramic [28]. Noguchi et al. [29] considered that the lattice distortion of the TaO_6 octahedra along *a*-axis played a crucial role in the determination of E_c for SBT. The E_c lowers with smaller tilt angle along *a*-axis (α_x). Since T_c is dependent on the lattice distortion, there exists a relationship between T_c and E_c. Irie et al. also reported that E_c becomes larger in BLSFs with a higher T_c [8]. In present report, T_c decreases with the *Ln*-doping, which is likely responsible for the decrease of the E_c.

4. Conclusion

In the present report, the dielectric and ferroelectric properties of SB*Ln*T were investigated. The T_c of the samples shifts to lower temperatures monotonously with *Ln*-doping. The $2P_r$ increases at first, then decreases with the increase of lanthanide content. The variation of ferroelectric properties of SB*Ln*T is likely dominated by the competition of the decrease of oxygen vacancy concentration and the relief of the structural distortion. The ferroelectric property of $Sr_2Bi_4Ti_5O_{18}$ is obviously improved by La, Nd, Sm, or Dy-doping with appropriate content.

Acknowledgments

The authors would like to acknowledge the financial support by the National Natural Science Foundation of China (Grant no. 10274066). This work is sponsored by Innovation Project for Graduate Students from Education Bureau of Jiangsu Province.

References

[1] J.F. Scott, C.A. Araujo, Science 246 (1989) 1400.
[2] Auciello, J.F. Scott, R. Ramesh, Phys. Today 22 (1998).
[3] B.H. Park, B.S. Kang, S.D. Bu, T.W. Noh, J. Lee, W. Jo, Nature 401 (1999) 683.
[4] J.J. Lee, C.L. Thio, S.B. Desu, J. Appl. Phys. 78 (1995) 5073.
[5] H.D. Chen, K.R. Udayakumar, C.J. Gaskey, L.E. Cross, Appl. Phys. Lett. 67 (1995) 3411.
[6] H. Watanabe, T. Mihara, H. Yoshimori, Carols A. Paz de Araujo, Jpn. J. Appl. Phys. 34 (1995) 5240.
[7] H. Irie, M. Miyayama, T. Kudo, J. Appl. Phys. 90 (2001) 4089.
[8] D.J. Taylor, R.E. Jones, P. Zurcher, P. Chu, Y.T. Lii, B. Jiang, S.J. Gillespie, Appl. Phys. Lett. 68 (1996) 2300.
[9] S.T. Zhang, C.S. Xiao, A.A. Fang, B. Yang, B. Sun, Y.F. Chen, Z.G. Liu, Appl. Phys. Lett. 76 (2000) 3112.
[10] Y. Noguchi, I. Miwa, Y. Goshima, M. Miyayama, Jpn. J. Appl. Phys. 39 (2000) L1259.
[11] Y. Noguchi, M. Miyayama, Appl. Phys. Lett. 78 (2001) 1903.
[12] U. Chon, K.B. Kim, H.M. Jang, G.C. Yi, Appl. Phys. Lett. 79 (2001) 3137.
[13] R.D. Shannon, Acta. Cryst. A 32 (1976) 751.
[14] J. Zhu, W.P. Lu, X.Y. Mao, R. Hui, X. B Chen, Jpn. J. Appl. Phys. 42 (2003) 5165.
[15] M. Osada, M. Tada, M. Kakihana, T. Watanabe, H. Funakubo, Jpn. J. Appl. Phys. 40 (2001) 5572.
[16] J. Zhu, X.-B. Chen, Z.-P. Zhang, J.-C. Shen, Acta Mater. 53 (2005) 3155.
[17] J. Zhu, X.-B. Chen, J.-H. He, J.-C. Shen, J. Solid State Chem. 178 (2005) 2832.
[18] Y. Noguchi, H. Shimizu, M. Miyayama, K. Oikawa, T. Kamiyama, Jpn. J. Appl. Phys. 40 (2001) 5812.
[19] K. Srinivas, A.R. James, J. Appl. Phys. 86 (1999) 3885.
[20] R.R. Das, P. Bhattacharya, W. Perez, R.S. Katiyar, Appl. Phys. Lett. 81 (2002) 4052.
[21] S. Gopalan, C.-H. Wong, V. Balu, J.-H. Lee, J.H. Han, R. Mohammedali, J.C. Lee, Appl. Phys. Lett. 75 (1999) 2123.
[22] Z.H. Bao, Y.Y. Yao, J.S. Zhu, Y.N. Wang, Mater. Lett. 56 (2002) 861.
[23] Y. Shimakawa, Y. Kubo, Y. Nakagawa, S. Goto, T. Kamiyama, H. Asano, F. Izumi, Phys. Rev. B 61 (2000) 6559.

[24] Y. Noguchi, M. Miyayama, T. Kudo, J. Appl. Phys. 88 (2000) 2146.
[25] Y. Noguchi, M. Miyayama, T. Kudo, Phys. Rev. B. 63 (2001) 214102.
[26] G.L. Miessler, D.A. Tarr, Inorganic Chemistry, Prentice-Hall, Englewood Cliffs, NJ, 2004, p. 38.
[27] W.P. Lu, X.Y. Mao, X.B. Chen, J. Appl. Phys. 95 (2004) 1973.
[28] X. Wang, H. Ishiwara, Appl. Phys. Lett. 82 (2003) 2479.
[29] Y. Noguchi, M. Miyayama, K. Oikawa, T. Kamiyama, J. Appl. Phys. 95 (2004) 4261.